ELECTROLUMINESCENCE INVESTIGATION ON THIN FILM MODULES

Thomas Weber, Anton Albert, Nicoletta Ferretti, Margarete Roericht, Stefan Krauter* and Paul Grunow
Photovoltaik Institut Berlin AG, Wrangelstr. 100, 10977 Berlin, Germany
Phone: +49 30 814 52 64 111, Fax: +49 30 814 52 64 101, e-mail: weber@pi-berlin.com
*University of Paderborn, Institute of Electrical Engineering, Sustainable Energy Concepts, Pohlweg 55, 33098 Paderborn, Germany, Phone: +49 5251 60-2301, Fax: +49 5251 60-3235, e-mail: stefan.krauter@upb.de

ABSTRACT: The fast market growth during the recent years led to huge amounts of production capacities and a large variety of module types. The increasing need for cost reductions obliges the manufacturers to maximize production and module efficiencies. Electroluminescence investigation is a powerful tool to reveal failures of thin film photovoltaic modules during the production stage and within test sequences. We use it to identify failures after reliability tests included in the IEC 61646 or beyond such as bias damp heat assessments. In an earlier stage, the manufacturer could use it to sort and optimize his products directly after frontend production. The results presented here aim to pave the way for such an inline electroluminescence analysis.

In this paper we also present spectral analysis of electroluminescence signals to simplify the choice of cameras and filters as a set-up for an EL testing station. Furthermore, we compiled a failure catalogue for all thin-film modules, applying electroluminescence. We developed a brightness-evaluation sheet to describe the analogies between power losses and lowering of brightness. Finally, we investigated the effect of the shunt resistance of CIGS modules on their weak light behavior.

Keywords: electroluminescence, reliability, production yield.

1 INTRODUCTION

Since 2005 electroluminescence (EL) has been a well known method for characterization of photovoltaic devices [1]. Today, it is already possible to find on the market 20 equipment companies offering 88 different EL/PL inspection systems [2]. A wide spread of applications and R&D topics can be found from the publications of the working groups around the globe. The fundamentals for these applications are described in the work of Rau, who analysed the relation of the electroluminescence of solar cells as light emitting diodes to the quantum efficiency of photocarrier collection [3]. Distinguishing cells in an entire module by calculating the internal current-voltage curve of each cell is one aspect [4]. An analysis of the absorber quality and circuit uniformity has been also presented [5,6]. Furthermore, simulations were done to understand the impact of defects and inhomogeneities on the module performance [7]. Electroluminescence as diagnostic tool is also implemented in test laboratories and is used to reveal failures after production or stress tests [8-11]. Microscopic diagnostic were developed as well [12] and comparisons to other diagnostic tools were drawn [13].

Working out the special aspect of the shunt detecting with electroluminescence it was already described by Mack [7] that modules are not that affected as single devices. Furthermore, Helbig showed the ability of the EL-technique to “calculate the mean voltage over all cells of the module and the corresponding standard deviation to classify module performances” [4]. The origin of the shunts was described by Sugimoto [5] and Tsakmakes [6].

Since 2007 we use EL as laboratory technique for all PV modules at Photovoltaic-Institute Berlin. We worked on the development of a standard for the analysis of crystalline modules. Today, a failure catalogue and a standard for failure interpretation are extended for thin-films. This implies profound knowledge of module production, degradation processes and luminescence properties. To progress, we started a R&D project with reknown companies in Berlin, with whom we are working on the development of a standardized inline EL-system.

In this paper we present the first results of the failure catalogue, EL-spectra for all thin film technologies, EL results after biased damp heat and last but not least the impact of many shunts on the yield of a module.

2 EXPERIMENTAL RESULTS

2.1 Experimental setup

In our accredited test laboratory (ISO 17025) we are performing tests according to IEC 61646 [14], among others. Beyond IEC we are performing damp heat tests with bias voltages to simulate real field conditions. After these stress tests the modules are observed via EL. [8]

Electroluminescence has been performed using a Nikon D 700 camera with the IR-filter removed from the high-sensivity 12 Mpixel CCD-chip. A 50 mm f/1.4 high-precision IR-optimised optic from Zeiss has been applied. To get an EL-signal a current has been applied in forward bias to the module. The brightness of the electroluminescence signal is influenced by the quantum efficiency, dark current losses and band gap shifts of the cell.

The spectra of the electroluminescence signals are measured with the use of a calibrated Tec-5 multichannel diode spectrometer. A MCS-CCD sensor with sensitivity in the wavelength range from 200 nm to 980 nm and an InGaAs sensor with a range between 900 nm and 1,700 nm have been used.

2.2 EL Failure Catalogue

In the following, we distinguish between features in the EL image which are related to power losses (failures) and features without power losses (flaw). We observe also the reversible effects, which show recovering of power losses after the biasing, similar to the polarisation effect on crystalline silicon modules (now called PID = potential induced degradation) [11]. Table 1 lists the features with power losses as failures and gives the possible root cause.

Table 1: Thin-film electroluminescence failure catalogue.

Failure/flaw	*root cause (test, where the failure can occur)*
Lightning	Bad or missing edge isolation, bad edge delete (DH, BDH)
Inhomogeneities	Fluctuations in thickness or stoichiometry results in fluctuation of the band gap. Impurities and grain boundaries reacts as recombination centers (initial, BDH)
R_{sh} decrease (shunting)	Impurities, bad or missing laser scribes or isolation trenches (DH, BDH)
R_S increase	Water ingress, corrosion (DH, BDH)
Reversible effects	Charge coupling (BDH)
Glass breakage	(ML, Hot-spot, Reverse Current Overload)
Dots from Hot-Spot test	Locally high temperatures (Hot-spot)
Light stabilization	After UV and LS, EL signal decreases stronger than P

DH = damp heat at 85°C and 85% relative humidity
BDH = DH with bias, ML = mechanical load test

In the following we show exemplary pictures and descriptions of some failures.

- Lightning (all types)

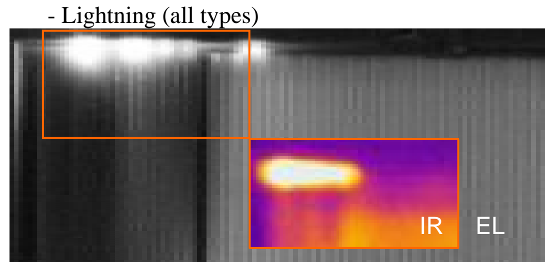

Figure 1: Part of a module with brightning effect due to damaged edge insulation. EL- and IR-picture show power losses via radiative heat.

Thin film modules are vulnerable at the edges and must be well water tightened. If damage of the edge isolation (delamination of encapsulant or sealant) occurs, water ingress might destroy the circuit of the surrounding cells. The module in Fig. 1 shows brightning at the module top left side and at the bottom due to strong shunt resistance decrease after 168 h DH. In consequence, the photo-voltage drops locally, which leads to a decrease in the electroluminescence signal of the cells. Mainly radiative heat is emitted in this area, which can be also detected via IR-imaging. Another reason for brightning might be an incorrect edge-deletion, which results in high leakage currents giving the same effect in the EL image.

- Inhomogeneties (CIS, CIGS, CdTe)

Inomogeneties in CIGS thin film modules are explained by band gap fluctuations in [15] limiting the cell efficiency. If these leads to lower collection efficiencies and/or higher losses in the IV curve this becomes visible in the electroluminescence signal as is well established for crystalline silicon. Additionally, fluctuations in the band gap will shift the luminescence spectra, which result in intensity variations, because of the limited sensitivity of the CCD camera in the infrared (s. Fig. 3). Fig. 2 shows an untreated CIGS module which reveals inhomogeneous luminescence on a larger scale. We compared the luminescence spectra of the "normal" emitting areas (A) to the weak emitting areas (B) and we could observe an intensity drop (2b) and a spectral shift (2c). Taking into account that the silicon sensor of our EL-camera detects only signals up to 100 nm, the lowering of the EL-signal (2a) can be attributed mainly to the intensity decrease. In this case the effect of the spectral shift can be neglected.

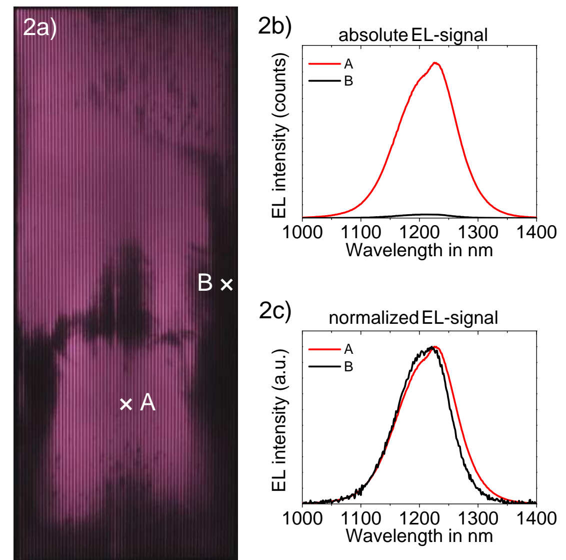

Figure 2: Module with inhomogeneous EL-signal (2a). The spectral measurement points for a normal EL-signal (A) and a weak EL-signal (B) are marked. 2b) shows the absolute measured EL-spectra and 2c) the normalized EL-spectra.

- R_{sh} decrease (shunting)

The shunt detection and differentiation after production is already well known and described by [5,6]. DH and BDH are known to increase the shunt content of CIGS modules. More information to the shunt detection can be found in the described literature and part 2.5.

2.3 Electroluminescence spectra

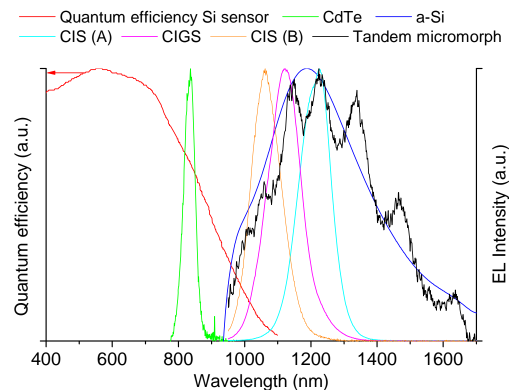

Figure 3: Electroluminescence spectra of the main thin film technologies in comparison to the quantum efficiency of a Si-sensor.

The spectra of the electroluminescence signals measured with the use of a tec5 multichannel diode spectrometer for the main thin film technologies are shown in Fig. 3. The CdTe signal has been measured with a MCS-CCD sensor with sensitivity in the wavelength range from 200 nm to 980 nm. In the case of CIS, micromorph tandem, CIGS and a-Si technologies an InGaAs sensor with a range between 900 nm and 1700 nm has been used.

The maximum of the CdTe and CIGS signal corresponds to the value reported in literature [16]. Two CIS modules of two different producers (A and B) have been measured. The difference in the peak position can be related to a difference in the material stoichiometry. The broad distribution of amorphous silicon between 940 and 1700 nm corresponds well with the spectrum in the literature, e.g. Fig. 5 in [17]. The interference fringes for the micromorph top cell point on a poorer TCO texturisation for the tandem module. The signal of the µ-crystalline bottom cell at 1100 nm is hidden by the broad signal of the amorphous silicon top cell.

The most popular camera in use for electroluminescence measurements are still based on Si sensor, because of their high spatial resolution, 12Mpixel in this work. Fig. 3 shows only a small overlap between the quantum efficiency of the Si-sensor and the EL emission spectrum of CIGS and amorphous/micromorph silicon. This explains the low EL intensities that we achieve on both materials, while the signal for CdTe is much better.

To improve the quality of electroluminescence measurements, a camera with an InGaAs sensor with quantum efficiencies up to 1700 nm should be used. Unfortunately, InGaAs cameras offer less spatial resolution at higher costs.

2.4 Brightness evaluation

The investigated modules have been exposed to 100 h and 500 h damp heat atmosphere (DH) at 85°C and 85% relative humidity at negative and positive bias of ±1000V vs. ground. Table 2 summarizes the samples and settings. The power losses have been determined with a sun simulator (Class AAA flasher Pasan SSIIIb 3m x 3m) and were compared to the brightness of the electroluminescence images taken with the CMOS camera above. CIGS-modules were photographed at $J = 40$ mA/cm² using 30 s of shutter time and a sensibility of ISO 1600. For the a-Si/µc-Si-modules $J = 40$ mA/cm² shutter time of 120 s and ISO 1600 have been used. We fixed the EL-settings in order to compare the initial condition to the BDH exposure after 100 h and 500 h. Temperature effects have been excluded by keeping the camera and the modules at constant temperatures [8]. The brightness values of the EL-pictures have been calculated from the sum of the brightness values of the single pixels.

Table 2: Overview of modules and BDH-settings under investigation for brightness evaluation.

Type	Technology	Applied Voltage
A	CIGS	-1000 V
B	CIGS	-1000 V
C	CIGS	+1000 V
D	a-Si/µc-Si	-1000 V
E	a-Si/µc-Si	-1000 V
F	a-Si/µc-Si	-600 V

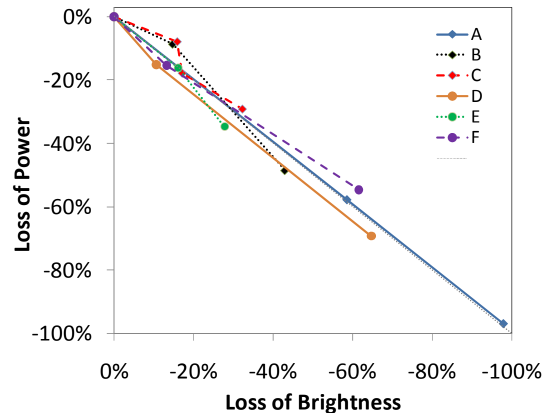

Figure 4: Brightness evaluation of biased DH-modules. The loss of brightness is visualized over the loss of power.

In Fig. 4 is shown how the performance of six modules is related to the loss of brightness. Beside the fact, that all thin film modules under investigation degrade strongly under BDH conditions (both plus and minus 1000V), we could find a linear dependency between loss of brightness and loss of power. As after damp heat short circuit current and open circuit voltage remained constant, the power losses account to fill factor losses only. This indicates dark current and series resistance losses. A huge potential is seen in this measurement method for process improvements in the production due to the fact that power losses can be spatially resolved in the EL images. Moreover, module degradation experiments and their result interpretation can profit from the relation of power determination and electroluminescence.

2.5 Shunt and Weak-Light Performance

Figure 5: EL pictures of a part of a CIGS module (Y). The upper image (A) has been recorded using an injection current density of $J = 40$ mA/cm² and for the buttom (B) image $J = 10$ mA/cm² has been applied. “A” reveals many shunts shown as dots, wheras “B” shows a pronounced quenching of the EL signal around the shunts.

This chapter aims to evaluate the influence of shunts on weak light performance and in consequence on the relative energy yield of a PV system. To investigate the effects of shunts we analysed five CIGS modules, which are prototypes. In a first step we recorded I-V-curves at

1000, 800, 400, 200, 100 and 50 W/m² and after EL. The modules were not pre-treated. From the I-V-curves we determined the slope near I_{sc} as a measure for the shunt resistance (R_{Sh}*). It results that the value for the shunt resistance decreases with the number of shunts in the EL image. For lower irradiances R_{sh}* was found to increase and furthermore increasing in dependence of the number of shunts (s. Fig. 6). Furthermore, decreasing current shows a quenching of the luminescence around the shunt and therefore underlines the measured effect in Fig. 6. In the first picture of Fig. 5 we used an injection current density of $J = 40$ mA/cm². Many shunts are visible as dots, whích is helpful for localization. Strong shunts show already a small blooming effect. Recording the same module with $J = 10$ mA/cm² and adjusting ISO setting and exposure time, a pronounced blooming effect becomes visible. The correlations in the work of Rau [3] show that the information given in EL has a direct impact on the shunt behavior of a module and therefore on the yield of a module.

Next, we calculated the efficiencies from the measured I-V-curves. Figure 7 shows the calculated efficiencies in dependence of the irradiance. At 100 W/m² the efficiency drop varies from -18 % (V) to -26 % (Z). This indicates a bad weak light efficiency in general and shows a dependency of the number of shunts to the weak light performance. The resulting efficiency drop under weak light conditions influences the yield of a module and PV-system. Comparing to the standard value of crystalline silicon of -10% at 100 W/m² and a -0.5 % yield drop per percent deviation, one can conclude a yield loss from 4 % to 8 % for Berlin.

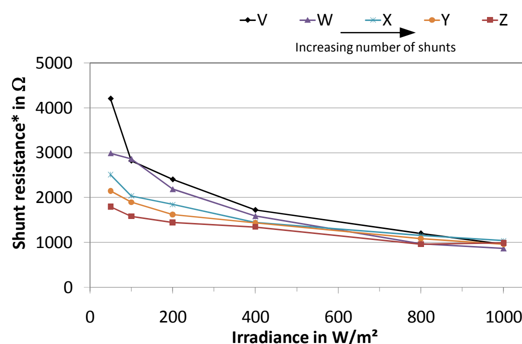

Figure 6: Shunt resistance* determined over the irradiance**.** Module V has a low shunt density and module Z a high shunt density.

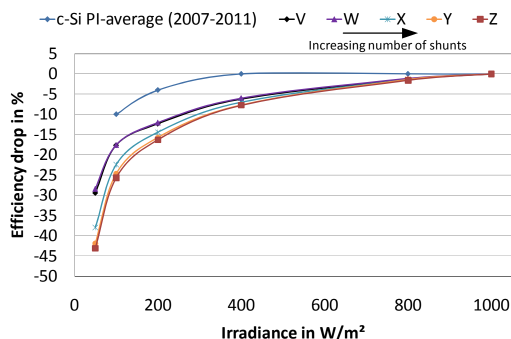

Figure 7: Efficiency drop for the investigated CIGS modules.

All thin film technologies are suffering from a high shunt number and the resulting yield decrease. Nevertheless thin film technologies, module types and even modules of the same type can very widely in their weak light performance. This method is usable to determine an expression for the number of shunts in a module, sorting them after production and enables to eliminate shunts.

3 CONCLUSION

Electroluminescence investigation is a powerful tool to reveal failures of thin-film photovoltaic modules during the production stage and during testing. In this work first results of a failure catalogue are presented and will be developed further. Spectral electroluminescence analysis shows need of InGaAs sensors with higher resolution for a better detection of thin-film technologies, except CdTe. The brightness evaluation presented here shows direct relation between power loss and brightness loss. Finally, a high density of shunts on thin-film modules shows a strong yield impact due to weak light efficiency drop.

ACKNOWLEDGEMENT

This study was supported by a grant from the European Union in the European Regional Development Fund. The authors are grateful to B. Rech, F. Ruske, J. Eberhardt and O. Vetterl for discussions and arguements.

4 REFERENCES

[1] T. Fuyuki et al. “Probeless detection of diffusion length mapping and defect distribution in polycrystalline silicon solar cells by photographic surveying” 20th EUPVSEC, Barcelona (2005), p.667.

[2] S.K. Chunduri, Photon International 01-2011, p. 158.

[3] U. Rau “Reciprocity relation between photovoltaic quantum efficiency and electrloluminescence emission of solar cells” Phys. Rev. B 76, 085303 (2007).

[4] A. Helbig et al. “Quantitative electroluminescence alanlysis of resistive losses in Cu(In, Ga)Se_2 thin-film modules” J. Solar Energy Materials & Solar Cells 94 (2010) 979-984.

[5] H. Sugimoto et al. “Impact of Cu(InGa)$(SeS)_2$ absorber quality and circuit uniformity on improved efficiency; application of photoluminescence and electroluminescence techniques” 24th EPVSEC, Hamburg (2009), p.2465

[6] E. Tsakmakis et al. “Influence of shunts on the performance of micromorph silicon thin film Modules”, 26th EPVSEC, Hamburg (2011).

[7] P. Mack et al. ”2D-Network Simulation and Modelling of CIGS Modules“ 25th EPVSEC, Valencia (2010), p.2877.

[8] T. Weber et al. “Electroluminescence on the TCO corrosion of thin film modules”, 25th EPVSEC, Valencia (2010), p.3169.

[9] R. Ebner et al. “Defect analysis in deiferent photovoltaic modules using electroluminescence (EL) and infrared (IR)-Thermography”, 25th EPVSEC, Valencia (2010), p.333.

[10] S. Koch et al. “Dynamic mechanical load tests on crystallinge silicon modules”, 25th EPVSEC, Valencia (2010), p.3998.

[11] S. Koch et al. “Polarisation effects and tests for crystalline silicone cells”, 26th EPVSEC, Hamburg (2011).

[12] M Boostandoost et al. “Microscopic characterization of thin-film crystalline silicon solar cells by electroluminescence and infrared LBIC”, 25th EPVSEC, Valencia (2010), p.3556.

[13] K. Zajac et al. “Investigation on flexible thin film solar cells using lock-in thermography and electroluminescence”, 25th EPVSEC, Valencia (2010), p.3331.

[14] IEC 61646. Thin-film terrestrial photovoltaic (PV) modules – Design qualification and type approval. (2nd ed). IEC Central Office: 2008.

[15] J.H. Werner et al. „Efficiency limitations of polycrystalline thin film solar cells: case of $Cu(In,Ga)Se_2$, J. Thin Solid Films, 480-481 (2005) 399-409.

[16] H. Häberlin „*Photovoltaik - Strom aus Sonnenlicht für Verbundnetz und Inselanlagen“,* 2. electrosuisse (2010) p.710.

[17] D. Han et al, Phys Rev. B Vol. 55, No. 23 (1997) p. 55.